Effect of water on the transport properties of protic and aprotic imidazolium ionic liquids – an analysis of self-diffusivity, conductivity, and proton exchange mechanism

ARTICLE *in* PHYSICAL CHEMISTRY CHEMICAL PHYSICS · APRIL 2014

Impact Factor: 4.49 · DOI: 10.1039/c4cp00527a · Source: PubMed

3 AUTHORS, INCLUDING:

Negin Yaghini
Chalmers University of Technology
5 PUBLICATIONS **18** CITATIONS

SEE PROFILE

Anna Martinelli
Chalmers University of Technology
32 PUBLICATIONS **729** CITATIONS

SEE PROFILE

PCCP

PAPER

View Article Online
View Journal | View Issue

Cite this: *Phys. Chem. Chem. Phys.*, 2014, **16**, 9266

Effect of water on the transport properties of protic and aprotic imidazolium ionic liquids – an analysis of self-diffusivity, conductivity, and proton exchange mechanism†

N. Yaghini, L. Nordstierna and A. Martinelli*

Received 5th February 2014,
Accepted 18th March 2014

DOI: 10.1039/c4cp00527a

www.rsc.org/pccp

In this paper we report on the transport properties of protic and aprotic ionic liquids of the imidazolium cation ($C_2C_1Im^+$ or C_2HIm^+) and the $TFSI^-$ or TfO^- anion as a function of added water. We observe that the self-diffusion coefficient of the ionic species increases upon addition of water, and that the cation diffuses faster than the anion in the entire water concentration range investigated. We also observe that the overall increase of anionic and cationic diffusion coefficients is significant for C_2HImTfO while it is rather weak for C_2C_1ImTFSI, the former being more hydrophilic. Moreover, the difference between cationic and anionic self-diffusivity specifically depends on the structure of the ionic liquid's ions. The degree of ion–ion association has been investigated by comparing the molar conductivity obtained by impedance measurements with the molar conductivity calculated from NMR data using the Nernst–Einstein equation. Our data indicate that the ions are partly dissociated ($\Lambda_{imp}/\Lambda_{NMR}$ in the range 0.45–0.75) but also that the degree of association decreases in the order C_2HImTfO > C_2HImTFSI ≈ C_2C_1ImTfO > C_2C_1ImTFSI. From these results, it seems that water finds different sites of interaction in the protic and aprotic ionic liquids, with a strong preference for hydrogen bonding to the –NH group (when available) and a stronger affinity to the TfO anion as compared to the TFSI. For the protic ionic liquids, the analysis of ^{1}H NMR chemical shifts (upon addition of H_2O and D_2O, respectively) indicates a water–cation interaction of hydrogen bonding nature. In addition, we could probe proton exchange between the –NH group and deuterated water for the protic cation, which occurs at a significantly faster rate if associated with the TfO anion as compared to the TFSI.

1 Introduction

During the last few decades ionic liquids (ILs) have attracted considerable attention due to their unique properties such as negligible vapor pressure, non-flammability, low melting point, and wide windows of thermal and electrochemical stability. The areas for ionic liquid applications are many and include dissolution of cellulose, nuclear fuel processing and organic reactions, among others.[1] While the non-volatility of ILs is interesting in organic syntheses offering a means to reduce the use of volatile organic compounds (VOC), the non-reactivity towards many acids and bases have made ILs very interesting compounds for use in green chemistry.[1] ILs are exceptionally good solvents, able to dissolve both organic and inorganic compounds and, by having very low melting points, they can be used in many chemical processes where the reaction products and the solvent can readily be separated and recycled, as in the case of biodiesel production.[2] The low emission policy adopted in many countries in the last few years has definitely contributed in highlighting ionic liquids as the future solvents for sustainable chemical processes.

In particular, ILs are widely investigated as electrolytes for energy conversion devices like the lithium-ion battery and the fuel cell.[1] In the former, non-flammability is the crucial property whilst in the latter non-volatility brings along a main advantage with respect to the issues of dehydration and thus reduced operational temperature, encountered with hydrated Nafion membranes.[3] In fact, the use of protic ILs (PILs) in fuel cells allows for operational temperatures higher than 120 °C,‡ hence reducing the amount of the platinum catalyst at the

Applied Surface Chemistry, Department of Chemical and Biological Engineering, Chalmers University of Technology, 412 96 Gothenburg, Sweden.
E-mail: anna.martinelli@chalmers.se, yaghini@chalmers.se

† Electronic supplementary information (ESI) available. See DOI: 10.1039/c4cp00527a

‡ This is also the target set by the U.S. Department of Energy (DOE) to promote the implementation of intermediate-temperature fuel cells in, for instance, the transport sector.

electrodes and enhancing the overall fuel cell efficiency.[4–6] However one should consider that as a result of the electrochemical reaction at the cathode, water is produced that can back-diffuse into the membrane and mix with the electrolyte. Hence, from the viewpoint of real fuel cell applications it is crucial to understand not only the properties of PILs, but also those of H_2O–PIL mixtures. Although water has long been considered an undesired impurity that affects the properties of ionic liquids, more recently the approach to deliberately add water to ILs has increased significantly.[7] Therefore, the issue of understanding the chemical and physical properties of H_2O–IL binary systems in the entire composition range has come to the attention of several researchers.[7–11] Nevertheless, since this is an emerging field of research, many issues are still unclear and vigorously debated.

From the studies reported so far, it seems that water mainly binds to the anion[12,13] but we believe that this must also depend on the basicity of the anion considered. Perfluorinated anions like bis(trifluoromethanesulfonyl)imide (TFSI) and triflate (TfO) are poorly basic and thus expected not to strongly interact with water; however it has been reported that the strength of hydrogen bond between water and triflate (TfO) is slightly higher than that of TFSI.[12,13] Although aprotic ILs like C_2C_1ImTFSI have been reported to be immiscible with water,[1,7,14] the protic counterpart can promote water miscibility. C_2C_1ImTfO and C_2HImTfO, on the other hand, are both totally miscible with water. The issue of miscibility and hydrophilicity in the IL–water mixtures has to date not been addressed extensively. A general result, however, is that longer alkyl chains on the cation reduce hydrophilicity. Furthermore, Kohno *et al.*[15] found that while $[N_{4444}]^+$ based ionic liquids associated with $[TsO]^-$, $[DMBS]^-$ or $[CF_3COO]^-$ are miscible with water, the $[P_{4444}]^+$ analogues undergo LCST-type phase transition.[15] As also discussed by Kohno *et al.*[7] "*The strength of the hydrogen bonding between ILs and water should also be capable of predicting the degree of hydrophobicity of ILs, which would be related to the energy of interaction between the ILs and water molecules.*[16]" However, this relationship may not be straightforward. In this context, a direct interaction between water and ammonium based cations is manifested by increased H-bonding.[17] On the other hand, the nature of interaction between water and imidazolium based ionic liquids has been investigated to a limited extent[18–21] and, to the best of our knowledge, no reports are available on the effect of added water on the ionic mobility in imidazolium ionic liquids.

In this study we thoroughly investigate the transport properties in a series of imidazolium based ionic liquids, where the cation is varied from aprotic to protic and the anion from less to more hydrophilic. By employing pulsed field gradient nuclear magnetic resonance (PFG NMR) spectroscopy we investigate to what extent water promotes the mobility of different molecular species and, in this context, the influence of cationic protonation and anionic hydrophilicity. A wide range of water-to-IL compositions is analyzed and, where relevant, the mechanism of proton exchange is also investigated. In addition, to address the issue of ionic association the $\Lambda_{imp}/\Lambda_{NMR}$ ratio is analyzed, where Λ_{NMR} is calculated by applying the Nernst–Einstein equation to the self-diffusion coefficients obtained by PFG NMR, and Λ_{imp} is the molar conductivity independently obtained by impedance measurements.

2 Experimental

2.1 Material

1-Ethyl-3-methylimidazolium bis(trifluoromethanesulfonyl)imide (C_2C_1ImTFSI), 1-ethyl-3-methylimidazolium trifluoromethanesulfonate (C_2C_1ImTfO), 1-ethylimidazolium bis (trifluoromethanesulfonyl)imide (C_2HImTFSI) and 1-ethylimidazolium trifluoromethanesulfonate (C_2HImTfO) were purchased from IoLiTec, Germany, and stored in a glove box until use. The cationic and anionic molecular structures, along with the proton labeling used in this work, are shown in Fig. 1. H_2O–IL mixtures were prepared with different H_2O-to-IL molar ratios, x, with x varying in the range $0 \leq x \leq 1$. H_2O–IL samples were analyzed immediately after preparation.

2.2 PFG NMR

Pulsed field gradient nuclear magnetic resonance (PFG NMR) experiments were performed on a Bruker Avance 600 spectrometer. The stimulated echo pulse sequence[22] was employed to determine the self-diffusion coefficient of the molecular species. All diffusion measurements were performed at 30 °C, at which all samples are in the liquid state. The NMR tubes containing the liquids were thermally equilibrated for 30 minutes before the measurement. Self-diffusion coefficients were obtained

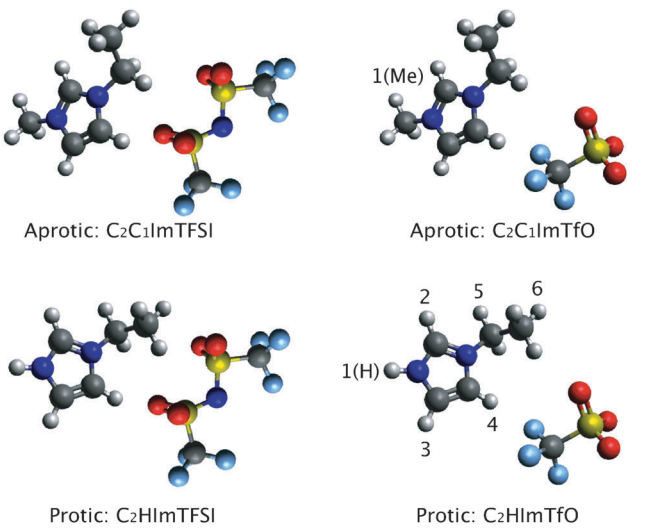

Fig. 1 Molecular structure and acronym for the investigated protic and aprotic ionic liquids: 1-ethyl-3-methylimidazolium bis(trifluoromethanesulfonyl)imide, C_2C_1ImTFSI (top left, A); 1-ethyl-3-methylimidazolium (trifluoromethanesulfonate), C_2C_1ImTfO (top right, B); 1-ethylimidazolium trifluoromethanesulfonate, C_2HImTfO (bottom right, C); and 1-ethylimidazolium bis(trifluoromethanesulfonyl)imide, C_2HImTFSI (bottom left, D). Proton labeling is also shown to distinguish between the protic, 1(H) and the aprotic 1(Me) sites, as well as aromatic and aliphatic protons.

by fitting the decay of the echo signal using the Stejskal–Tanner expression, $I = I_0 \exp\{-(\gamma\delta G)^2 D(\Delta - \delta/3)\}$, where I is the signal intensity, I_0 is the signal intensity of spin-echo at zero gradient, G is the gradient strength, D is the diffusion coefficient, δ the length of the gradient pulse, and Δ is the diffusion time. The applied linear gradient was varied in the range 0–1200 G cm^{-1}, while the diffusion time Δ and the pulse duration δ were set to 150 and 0.6 ms respectively. The number of acquisitions in each experiment was 16 and the relaxation delay was 12 s. To ensure that thermal convection did not affect our results, we run the diffusion NMR experiments for different Δ values (100, 150, and 200 ms) whereby the self-diffusion coefficients were observed not to depend on Δ. The magnetic field gradients were calibrated using a 50/50 mixture of HDO and D_2O.[23] The consistency of the measured diffusion coefficients from ^{1}H and ^{19}F PFG NMR experiments was verified using the reference sample trifluoroethanol (CF_3CH_2OH).

2.3 Proton exchange and chemical shift analyses

^{1}H NMR spectra were collected for proton exchange and chemical shift analyses on a Varian 400 MHz spectrometer using 5 mm NMR tubes with inserted capillaries filled with octamethylcyclotetrasiloxane as a chemical shift reference. In order to study the proton exchange between water and the ionic liquid, the D_2O–IL mixture was prepared at various concentrations.

2.4 Conductivity measurements

Conductivity measurements were performed on a CDM 210 conductivity meter instrument. Consistent with the procedure used for diffusion measurements, the samples were equilibrated for 30 minutes at 30 °C before collecting data. A dosimeter was used to carefully control the amount of water added to the ionic liquid. The instrument was calibrated with aqueous KCl at a concentration of 0.01 M.

3 Results and discussion

3.1 Effect of water on ionic mobility

Fig. 2 shows the single pulse ^{1}H NMR spectra of the four pure ionic liquids investigated. All proton resonances are well resolved wherefore the self-diffusion of different protons could be analyzed independently. Our analysis reveals that all imidazolium protons diffuse at the same rate, with a deviation of only 0.1–1.5 percent, hence we define the self-diffusion of the whole imidazolium molecule as the mean value obtained from the distinct proton resonances. Note that in Fig. 2 the resonance of the –NH proton is clearly visible for both C_2HImTFSI and C_2HImTfO, at 11.04 and 11.99 ppm respectively.

Fig. 3 shows the self-diffusion coefficients of the cation (D^+), anion (D^-), and water (D_{water}) in the four H_2O–IL binary systems.§ We observe that the diffusivity of all molecular species increases upon addition of water, which is rationalized

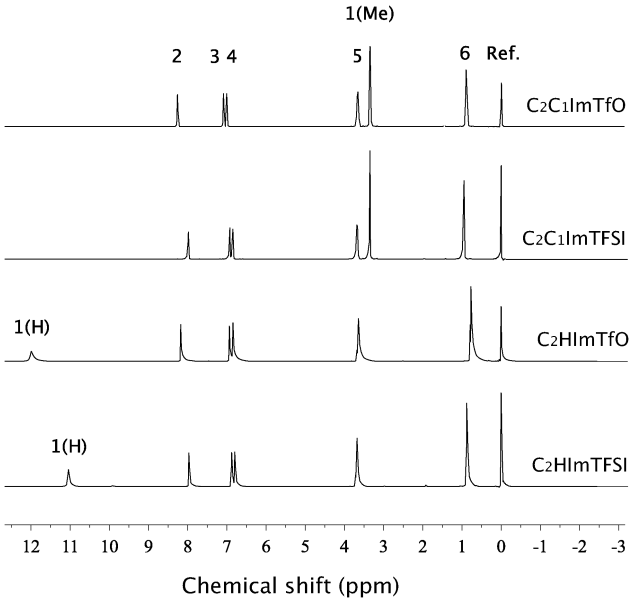

Fig. 2 Single pulse ^{1}H NMR spectra of the investigated pure ionic liquids. From bottom to top: C_2HImTFSI, C_2HImTfO, C_2C_1ImTFSI, and C_2C_1ImTfO. The proton resonance of the reference molecule octamethylcyclotetrasiloxane is also indicated. The assignment of NMR peaks is according to the labeling in Fig. 1.

by an overall decrease of viscosity. An increase in diffusivity with added water had already been observed for ethylmethylimidazolium ethylsulfate ($C_2C_1Im^+EtSO_4^-$) and ethylmethylimidazolium triflate ($C_2C_1Im^+TfO^-$), which apparently correlates with a decrease of the activation energy when self-diffusion is described by the Arrhenius equation as recently discussed by Menjoge *et al.*[19] Similar results have also been discussed for pyrrolidinium hydrogensulfate ($Pyrr^+HSO_4^-$), pyrrolidinum trifluoroacetate ($Pyrr^+CF_3COO^-$),[8] and ethylmethylimidazolium methanesulfate ($C_2C_1Im^+MeSO_3^-$).[8,19,21,24] Another observation is that the self-diffusivity in pure ionic liquids (*i.e.* at $x = 0$) is lower for the protic ionic liquids as compared to their aprotic analogues, which is consistent with their higher viscosity. It is also interesting to note that in the entire concentration range investigated the cation diffuses faster than the anion. This behavior has previously been observed in pure ionic liquids[19,24,25] and becomes an anomaly when the cationic size exceeds that of the anion. Indeed, according to the classical Stokes–Einstein relation larger molecules should diffuse slower than smaller molecules, and *vice versa*.¶ This relation does not hold in some ionic liquids,[25] which thus do not behave as classical hydrodynamic fluids. In this context, Tokuda *et al.* found that the c factor in the Stokes–Einstein relation must be assumed to be smaller than 6 to fit the experimental data from ionic liquids of the C_4C_1Im cation,[26] and that this factor is smaller for cations than for anions despite their similar

§ Note, however, that D_{water} is not necessarily the diffusion coefficient of water but that of the signal corresponding to water protons and other exchangeable protic protons in the system.

¶ According to the Stokes–Einstein relation, $D = kT/c\pi\eta r_s$,[26] where k is the Boltzmann constant, T is the absolute temperature, c is a constant (for spheres with stick boundary condition at infinite dilution equals to 6), η is the viscosity and r_s is the effective hydrodynamic (Stokes) radius.

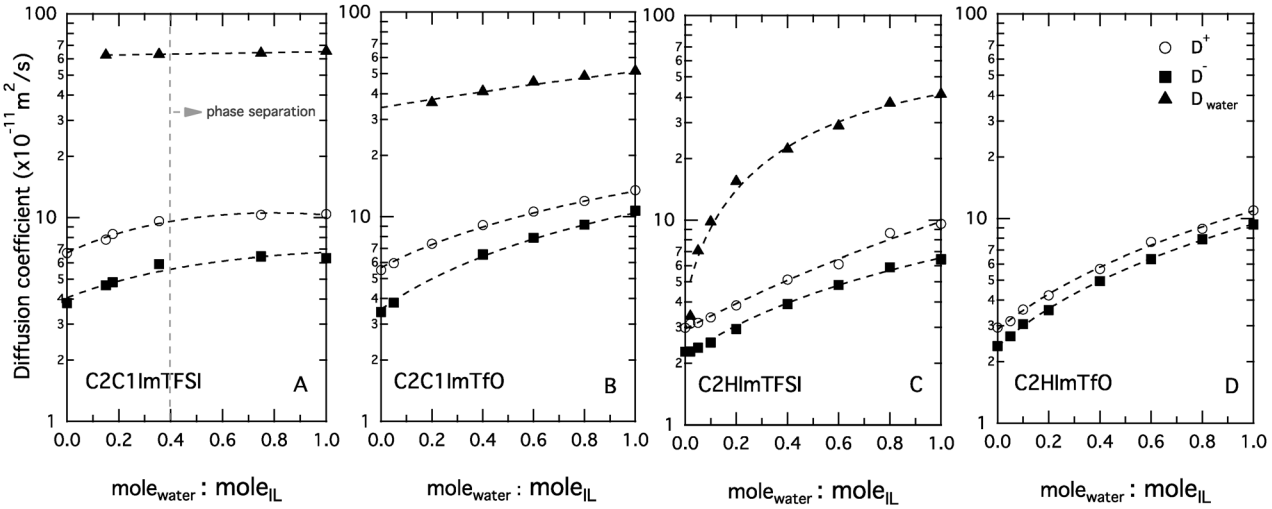

Fig. 3 Self-diffusion coefficients of cations (D^+, ○), anions (D^-, ■) and water (D_{water}, ▲) as a function of added water in the four investigated ionic liquids. (A) C_2C_1ImTFSI–water; (B) C_2C_1ImTfO–water; (C) C_2HImTFSI–water, and (D) C_2HImTfO–water. Dotted lines are guide to the eye.

van der Waals radii. This intriguing behavior has been ascribed to some degree of anisotropy in the cationic motion, with "*...the motion on the ring plane and almost perpendicular to the 1-alkyl chain being the less hindered one*".[27] The reported van der Waals radii for the ionic species considered in the present study are 0.303 nm ($C_2C_1Im^+$), 0.267 nm (TfO^+), and 0.327 nm ($TFSI^-$).[28] The radius for C_2HIm^+ is not reported in the literature but can be assumed to be comparable to, or smaller than, that of $C_2C_1Im^+$. So, from ionic radii considerations only, it is a 'hydrodynamic anomaly' that the C_2C_1Im and C_2HIm cations diffuse faster than their associated TfO anion.

As mentioned above, one effect of adding water to ionic liquids is the decrease of the self-diffusion activation energy, as revealed by MD simulations.[19] These simulations, however, also indicate that this decrease becomes less significant at higher water concentrations, more specifically at concentrations with more than 0.7 water molecules per cation:anion pair, *i.e.* for $x \geq 0.7$. In good agreement with these findings, we also observe that the effect of water on self-diffusion is stronger at lower concentrations and becomes weaker as more water is added. The behavior displayed in Fig. 3 by the system based on C_2C_1ImTFSI is slightly different from the others, with plateau values for D^+ and D^- observed for $x \geq 0.4$. Upon further addition of water there are no appreciable changes, which we attribute to the occurrence of phase separation due to the immiscibility of this aprotic ionic liquid with water. For C_2C_1ImTfO, which has a more water affine anion, the increase of both D^+ and D^- is observed in the whole concentration range, similarly to the cases of C_2HImTFSI and C_2HImTfO.

The issue whether proton transport in ionic liquids can occur *via* the Grotthuss mechanism is currently vividly debated, yet not conclusively verified. While Noda *et al.* claim that the proton conduction behavior in non-equimolar mixtures of imidazole and HTFSI follows a combination of Grotthuss- and vehicle-type mechanisms,[29] Blanchard *et al.* bring to the attention of researchers the possibility of an overestimation of self-diffusion values as a result of fast proton exchanges between water (impurities) and protic sites in the time-frame of the diffusion experiments.[30] Moreover, Anouti *et al.* also believe that the proton conduction in water-added pyrrolidinium (protic) ionic liquids can follow a combination of Grotthuss- and vehicle-type mechanisms, at least in the water-rich domain.[8] Achieving a unifying picture is made even more complicated by the fact that the above-mentioned studies concern ionic liquids of very different structures – imidazolium,[29] ammonium,[30] and pyrrolidinium.[8] Nevertheless, one method to assess the occurrence of the Grotthuss mechanism is to verify that the D_{NH}/D_{cation} ratio is significantly higher than unity.[29] In the present study, the D_{NH}/D_{cation} ratio for the C_2HImTFSI system is shown to be close to one at all water concentrations; see Table 1. This indicates that the main transport mechanism is of vehicular type and that the imidazolium cation keeps its native structure with an intact amine group, at least in time scale of the delay time in diffusion experiment, *i.e.* 150 ms. The latter observation is of key importance to the discussion below, since it tells that the only charges present in solution are the ionic liquid's cation and anion, excluding the formation of long-lived H_3O^+ ions. The D_{NH}/D_{cation} ratio for the C_2HImTfO system could not be calculated due to fast proton exchange during the time scale of the

Table 1 Excess self-diffusion values expressed as D_{NH}/D_{cation} as a function of added water for C_2HImTFSI

mole$_{water}$:mole$_{IL}$	D_{NH}/D_{cation}
0	1.01
0.02	1.01
0.05	1.01
0.1	0.99
0.2	1.00
0.4	1.00
0.6	0.95
0.8	0.98
1	N.A.

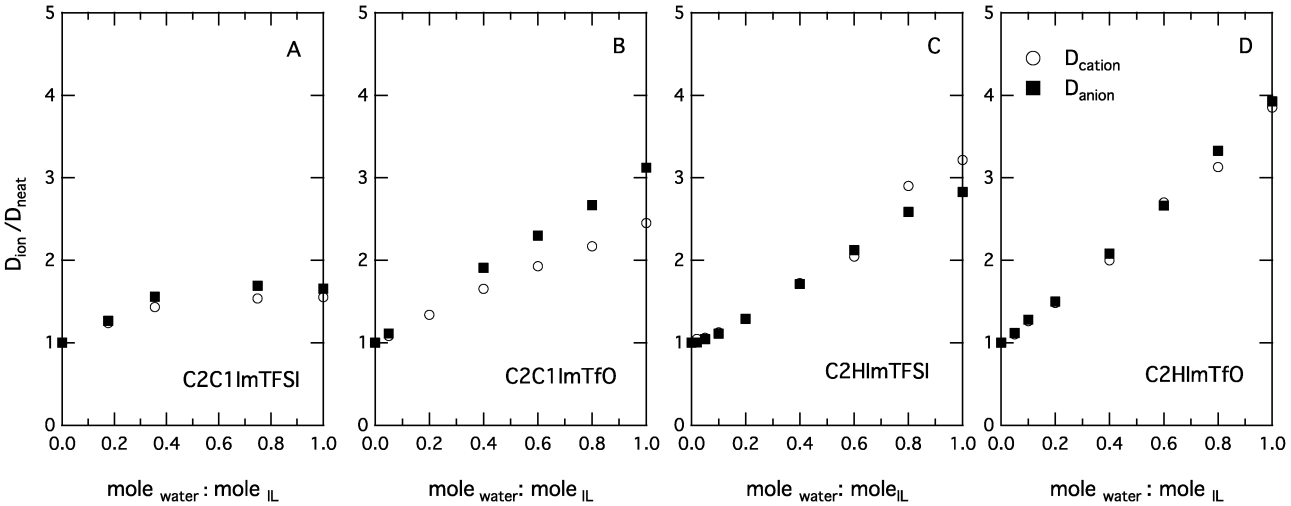

Fig. 4 Normalized self-diffusion coefficients with respect to the bulk values for the cation ($D^+/D_{neat}{}^+$, ○) and the anion ($D^-/D_{neat}{}^-$, ■) as a function of added water. Dotted lines are guide to the eye.

NMR experiment, wherefore the NMR signals of the –NH group and water are merged into one signal and D_{NH} cannot be analyzed independently.

A particularly interesting aspect in this context is the concentration dependence of the self-diffusion of water. It increases with x in the binary systems and by different amounts depending on the ionic liquid's structure.‖ D_{water} increases only slightly in C_2C_1ImTfO, while it depends much more strongly on the concentration in C_2HImTFSI. Indeed, as shown in Fig. 3C, water self-diffuses associatively to the C_2HIm cation at very low concentrations ($x < 0.1$). This associative behavior has not been reported before and may find a plausible explanation in a specific water–cation interaction. Nevertheless, upon addition of more water ($x \geq 0.1$) D_{water} increases steeply and water appears to self-diffuse at its distinct rate. For C_2HImTfO, the self diffusion of water could not be independently evaluated for any x value, due to the merged signals of the –NH group and water, as discussed above.

The different degrees to which the self-diffusion of cations and anions is affected by added water can be appreciated from the analysis of the D^+/D^- ratio, as also suggested by Stark *et al.*[21] In agreement with the results of Menjoge *et al.*[19] we also find that D^+/D^- steadily decreases upon addition of water in C_2C_1ImTfO, indicating that the cation is more affected than the anion. But here we also observe that this ratio is almost constant in C_2C_1ImTFSI and C_2HImTfO, while it increases in C_2HImTFSI for concentrations higher than $x \geq 0.6$ (see Fig. S1, ESI†). Nevertheless, to better understand the diffusional properties on a molecular level, we here propose to analyze the excess ionic diffusivity by expressing the relative self-diffusion coefficients, $D^+/D_{neat}{}^+$ and $D^-/D_{neat}{}^-$, as summarized in Fig. 4 (where D_{neat} is the self-diffusion coefficient measured in a pure ionic liquid). Even though an overall increase of D/D_{neat} is observed as a result of lower viscosity, more subtle differences can be appreciated that depend on the ionic liquid's molecular structure. The highest increase (four-fold) with respect to the neat ionic liquid is observed for C_2HImTfO, followed by C_2C_1ImTfO/C_2HImTFSI (three-fold), and C_2C_1ImTFSI (less than two-fold). For C_2C_1ImTFSI the effect is limited to concentrations of $x \leq 0.4$. Another small but intriguing feature is that while in the H_2O–C_2HImTFSI system with 1 : 1 concentration D_{cation} exceeds D_{anion} (Fig. 4C), the opposite is observed at analogous concentrations in the C_2C_1ImTfO system (Fig 4B).**

A plausible explanation of this effect may be that water interacts with the ionic liquid through specific sites, most probably through the –NH group in protic ionic liquids and through the $-SO_3$ in the TfO anion, which by a drag effect can in turn result in a selective self-diffusion enhancement.†† This speculation would also explain why D^+ and D^- are equally and more greatly enhanced in the ionic liquid C_2HImTfO, which offers both type of interaction sites. Our hypothesis is in line with recently reported MD simulations and experimental studies that reveal the possibility of water–anion hydrogen bonding. These studies reveal that while hydrophobic anions like TFSI are not most favorable for strong and directional hydrogen bonds,[14] those with a higher water affinity like TfO do show a tendency to form water–anion complexes.[7] While the nature of the water–anion interaction will be investigated in more detail in a separate work with focus on vibrational spectroscopy,‡‡ the issue of water–cation interaction is further discussed in the next sections.

3.2 Effect of water on chemical shift

To further investigate the nature of $H_2O\cdots$cation interactions we analyze the chemical shifts, δ (ppm), in the ^{1}H NMR spectra

‖ The self-diffusion coefficient of water does not change in C_2C_1ImTFSI for x greater than 0.4, since water and C_2C_1ImTFSI are immiscible.

** The reader should note that in C_2C_1ImTfO the deviation of D^- from D^+ is considerable in the whole concentration range, as opposed to the other three systems.

†† That the $-SO_3$ in TfO interacts with water is indicated by Raman spectroscopic data which will be presented in a separate paper.

‡‡ Yaghini *et al.*, in preparation.

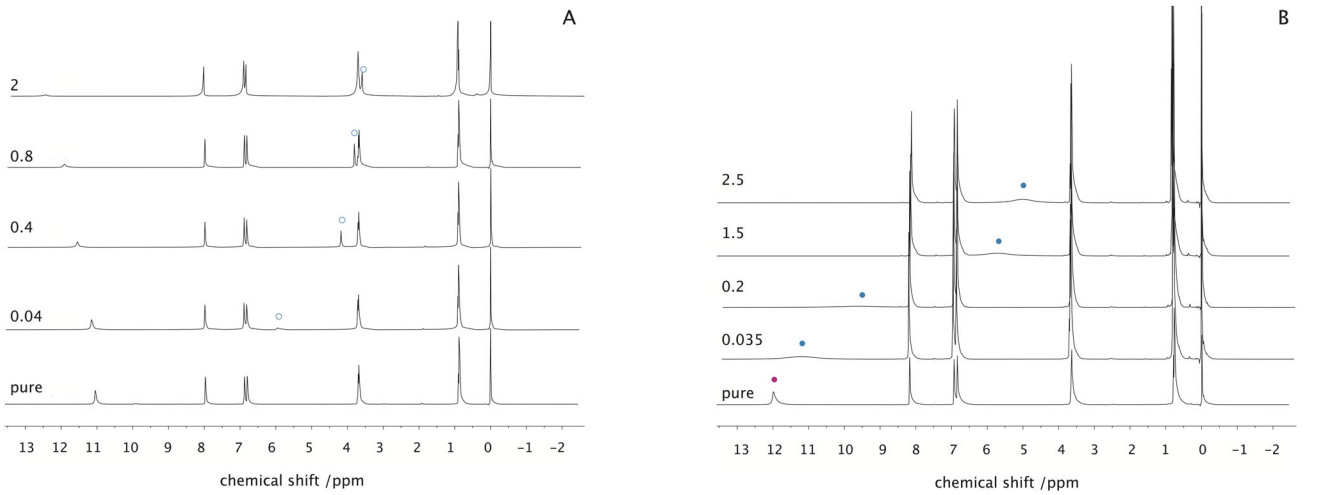

Fig. 5 ^{1}H NMR spectra of D_2O–C_2HImTFSI (A) and D_2O–C_2HImTfO (B) for different D_2O/IL molar ratios. The ^{1}H resonances assigned to DOH (or DOH–H_2O) are marked by circles.

of water–IL binary systems, see also Fig. S2 (ESI†). While the chemical shifts of imidazolium hydrogens (aromatic and aliphatic) and water insignificantly change upon addition of water to the aprotic C_2C_1ImTFSI and C_2C_1ImTfO based systems (Fig. S2A and B, ESI†), the chemical shifts of hydrogen in –NH and water (H_2O) considerably shift down-field and up-field, respectively, in C_2HImTFSI (Fig. S2C, ESI†). These shifts are a consequence of lower electron density (deshielding) for the –NH group and higher electron density (shielding) for water,[19,31] a clear evidence for a specific C_2HIm^+–water interaction through the –NH group, which we now can describe being of hydrogen bonding nature. The effect of hydrogen bonding on the chemical shift of the –NH proton has also been discussed previously for diethylmethylammonium trifluoromethanesulfonate (dema$^+$TfO$^-$)–water and imidazole–HTFSI non-equimolar mixtures.[9,29]

The scenario for C_2HImTfO is different (Fig. S2D, ESI†). The ^{1}H resonances of the –NH proton and water appear to be merged and broad at all water concentrations, wherefore the reported chemical shifts assigned to the –NH group are in fact an average of all –NH and water protons as these undergo fast exchange on the time scale for the NMR experiment. This merged peak continuously shifts up-field upon increased water content, while the chemical shift for the other imidazolium hydrogens remains unaltered.

3.3 Proton exchange

Having established the existence of hydrogen bonding between water and protic cations, we now investigate the proton exchange mechanism between these two molecular species. To this end, we analyzed the ^{1}H NMR spectra of D_2O–C_2HImTFSI and D_2O–C_2HImTfO systems for increasing D_2O concentrations, see Fig. 5A and B respectively. The chemical shift of the –NH group in C_2HImTFSI, $\delta_{1(H)}$, shifts down-field upon increasing D_2O content, consistently with the results obtained for the H_2O–IL systems. Moreover, the relative decrease of the ^{1}H NMR signal intensity assigned to –NH with increasing D_2O indicates the occurrence of complete proton exchange between the imidazolium protic site –NH and deuterated water. In fact, the complete exchange between –NH and D_2O in C_2HImTFSI occurs on a time scale longer than 0.5 ms,§§ in fact longer than 150 ms, which is the time scale of the diffusion experiment. In C_2HImTfO this proton exchange is so fast that the NMR signals associated with the –NH group and water are broad and merged for all D_2O concentrations investigated here, see Fig. 5B.

In Fig. 6 we summarize the chemical shift evolution as a function of added D_2O for the two protic ionic liquids. In C_2HImTFSI the chemical shift of the –NH proton, $\delta_{1(H)}$, shifts downfield and decreases in intensity upon addition of water, while the opposite is observed for the chemical shift of deuterated water, δ_{DOH}, Fig. 6A. This trend is in agreement with that shown in Fig. S2C (ESI†) and is attributed to a direct NH$\cdots$OD$_2$ (or ND$\cdots$OHD) interaction through hydrogen bonding.

The chemical shift and NMR intensity analyses of the D_2O–C_2HImTfO system reveal a slightly different scenario, Fig. 6B. The single broad and merged –NH/DOH ^{1}H resonance shifts up-field upon addition of D_2O (see also Fig. 5B) and its intensity evolution as a function of added D_2O also indicates a proton exchange between the C_2HImTfO cation and deuterated water. In this case, however, due to the merged character of the ^{1}H resonance, a quantitative estimation of the proton exchange would require further analyses, which is outside the scope of this work. We limit our discussion to the observation that the proton exchange between water and C_2HImTfO is much faster than in the analogues–C_2HImTFSI system, *i.e.* faster than 0.5 ms.

For a comparison of the state of water in different binary systems, the chemical shift of the ^{1}H resonance associated with water as a function of concentration is shown for all ionic liquids in Fig. 7. This plot reveals different states of water that

§§ This time is calculated as the inverse of the difference in chemical shift (in Hz) multiplied by the magnetic field strength.

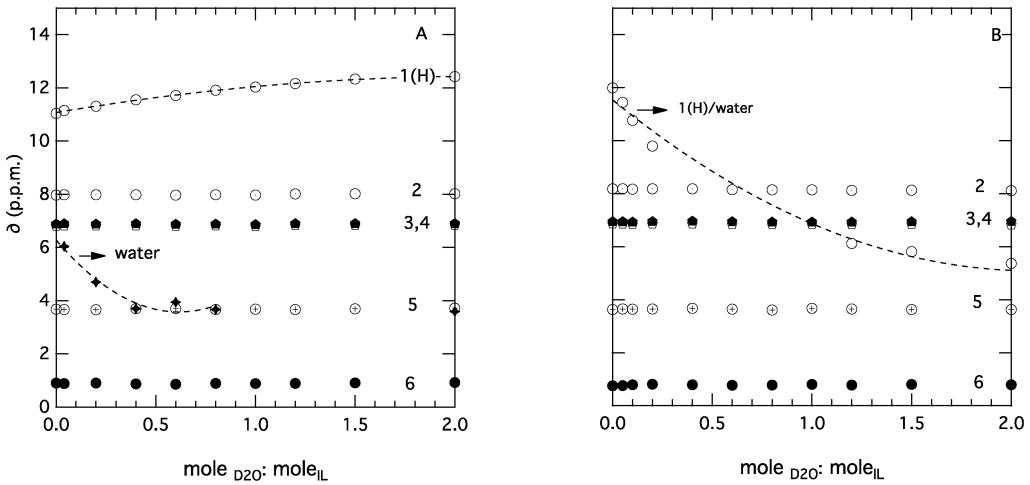

Fig. 6 (A) Chemical shift map of ^{1}H NMR experiments for D_2O–C_2HImTFSI and (B) D_2O–C_2HImTfO mixtures at different D_2O/IL molar ratios. Numbers "1(H), 2, 3, 4, 5, and 6" correspond to the NMR peaks of Fig. 2.

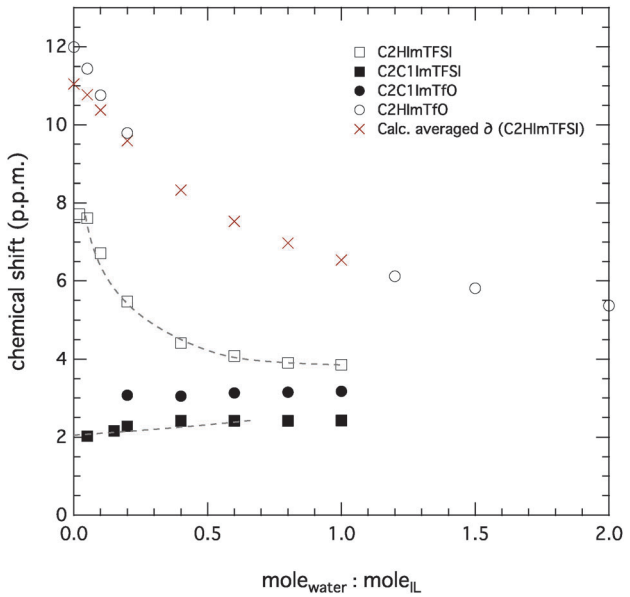

Fig. 7 State of water. The chemical shift of water as a function of added water in ILs is investigated. Given values for C_2HImTfO include the contribution of the –NH group. Calculated population averaged chemical shifts in C_2HImTFSI are indicated by red symbols.

depend on the surrounding cation:anion pairs. While δ_{H_2O} has a low value and is almost unaltered in aprotic ionic liquids, it is more concentration dependent in the protic ones. Indeed, at any concentration the chemical shift of water increases in the order C_2C_1ImTFSI < C_2C_1ImTfO < C_2HImTFSI < C_2HImTfO,¶¶ which is also the order in which hydrophilicity increases. This trend indicates that water is found in a more hydrogen bonded state in the protic ionic liquids as well as in the presence of the TfO anion, consistently with an increased hydrophilicity of the ionic liquid (see the order above). We can anticipate that this behavior is consistent with the frequency shift observed in the water sensitive range 3200–4000 cm^{-1} of infrared spectra (not shown here). This behavior also indicates a more intimate mixing of water with the protic ionic liquids, which is also reflected by self-diffusion values of water presented in Fig. 3. Here, the reader should recall that the chemical shift values given for C_2HImTfO in fact also include contributions from the –NH group. Thus, to qualitatively compare the state of water in the two protic ionic liquids we calculated the population averaged chemical shift for C_2HImTFSI, $\delta^{calc.} = p\delta_{water} + (1 - p)\delta_{NH}$, where p is the fraction of water protons in the system, *i.e.* $n_{water}/(n_{water} + n_{NH})$. The result is shown in Fig. 7 as red crosses. The good overlapping of the observed average chemical shift for C_2HImTfO with the calculated one for C_2HImTFSI indicates that the state of water in the two systems is very similar, and so should the proton exchange mechanism also be, the difference being mainly in the kinetics of the exchange process. We deduce that the faster exchange process observed for C_2HImTfO is induced by the TfO anion. In this respect, it is also interesting to note that as can be deduced from the chemical shifts in the pure ionic liquids (11.99 ppm in C_2HImTfO and 11.04 ppm in C_2HImTFSI), the proton in the –NH group is more 'acidic' when associated with the TfO anion. This difference can also explain the small but appreciable deviation between the observed and calculated averaged chemical shift curves at very low water contents, see Fig. 7.

3.4 Effect of water on ionic conductivity

In addition to the self-diffusion coefficients and the chemical shifts, we have also measured the ionic conductivity in order to achieve a more thorough picture of the transport properties in these water-added ionic liquid systems. The experimentally measured ionic conductivities are shown as a function of composition in Fig. 8.

At very low water concentrations ($x < 0.2$) the ionic conductivities in C_2C_1ImTFSI and C_2C_1ImTfO are comparable, and

¶¶ To remind, however, for the latter the chemical shift of water merged with that of –NH.

higher than those of C_2HImTFSI and C_2HImTfO (see Fig. 8A). The lower conductivity observed in the protic ionic liquid based systems qualitatively agrees with the trend observed from diffusion NMR experiments (see Fig. 3). Furthermore, while the ionic conductivity in C_2HImTFSI, C_2HImTfO, and C_2C1ImTfO based systems steadily increases with water concentration, that in C_2C_1ImTFSI shows no changes for $x > 0.4$ as a result of phase separation, and in agreement with the self-diffusion trend (see Section 3.1). Fig. 8 also shows that the relative increase in conductivity with respect to the neat ionic liquid ($x = 0$) is more enhanced for the TfO based ionic liquids. The overall increase in ionic conductivity with water content is in agreement with the data reported by Anouti *et al.* for the ionic liquids, ($PyrrHSO_4$) and ($PyrrCF_3COO$),[8] and has been tentatively attributed to a more dissociative character of the ionic species in solution.

However, the issue of ionic dissociation is more properly investigated by analyzing the molar conductivity ratio $\Lambda_{imp}/\Lambda_{NMR}$ also referred to as "ionicity", where Λ_{imp} is the molar conductivity obtained from impedance experiments and Λ_{NMR} is the molar conductivity calculated from NMR self-diffusion coefficients. Indeed, while impedance experiments probe the mobility of charged species only, by diffusion NMR any species in motion is detected regardless of its complexation state. Λ_{NMR} can be estimated from self-diffusion values using the

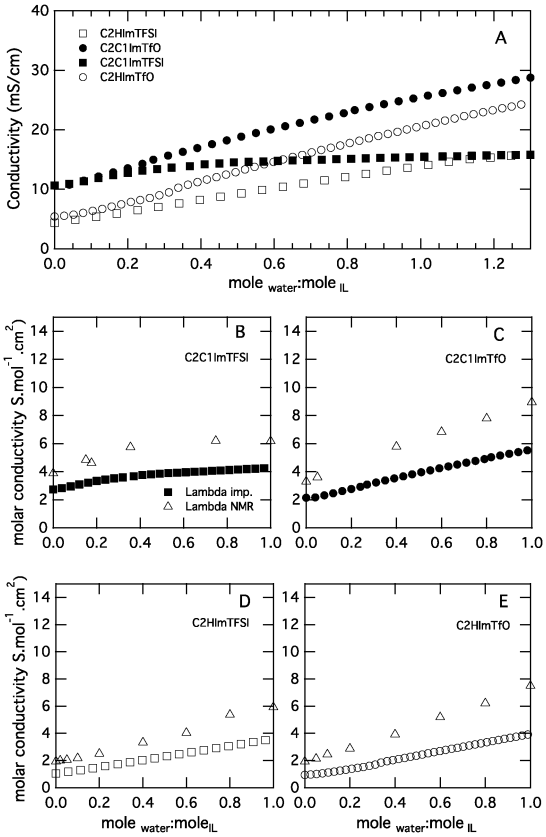

Fig. 8 (A) Ionic conductivity measured at 30 °C for the water added ionic liquids. (B–E) Concentration dependence of molar conductivity obtained from diffusion NMR and impedance measurements.

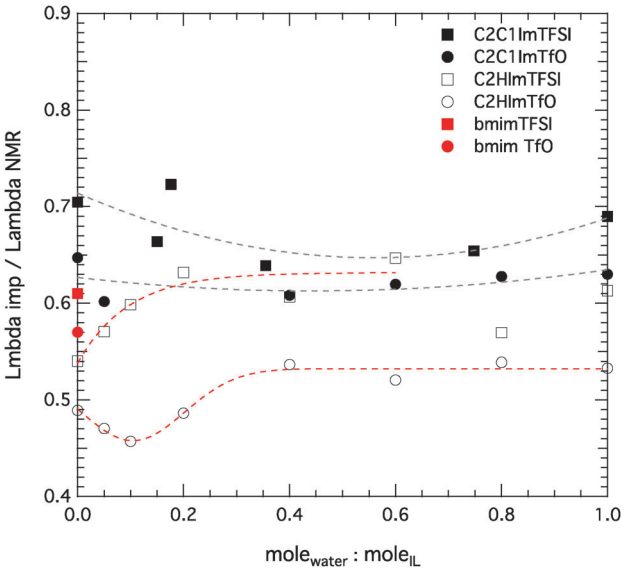

Fig. 9 Ionicity (expressed as $\Lambda_{imp}/\Lambda_{NMR}$) of the investigated ionic liquids as a function of added water. Ionicity values of pure C_4C_1ImTfO and C_4C_1ImTFSI are as reproduced from reference Tokoda *et al.* 2004 are also shown for comparison purpose. Dotted lines are guide to the eye only.

Nernst–Einstein (NE) equation, $\Lambda_{NMR} = (F^2/RT)\cdot(D_{cation} + D_{anion})$, where F is the Faraday constant and R is the universal gas constant.[32] The equation mentioned above is derived for non-interacting ions in infinite dilute electrolyte solutions, assuming that all ionic mobile species contribute to molar conductivity.[32] However, Harris *et al.*[33] and Hayamizu *et al.*[34] recently proposed a slightly modified form of this equation to better suit the complexity of electrolyte solutions and ionic liquids. Anyway, in the field of ionic liquids the $\Lambda_{imp}/\Lambda_{NMR}$ ratio is extensively used as an indicator of the degree of dissociation in ionic liquids.[35–37]

Fig. 8B–E show that Λ_{imp} is smaller than Λ_{NMR} in all ionic liquids at all water concentrations. A value of $\Lambda_{imp}/\Lambda_{NMR}$ smaller than unity (Fig. 9) means that part of the ionic species are associated and do not contribute to ionic conductivity. Interestingly, the ionicity in the investigated ionic liquids follows the order, C_2C_1ImTFSI > C_2C_1ImTfO ≈ C_2HImTFSI > C_2HImTfO, at least at very low (or zero) water concentrations. This trend is consistent with the results recently discussed by Tokuda *et al.* who observed that for identical cations the ionicity is higher for TFSI as compared to TfO.[26] The $\Lambda_{imp}/\Lambda_{NMR}$ values reported for the pure ionic liquids, C_4C_1ImTFSI and C_4C_1ImTfO,[26] are also shown in Fig. 9 for comparison (red symbols). This comparison shows that keeping the same anion, the ionicity is lower in $C_4C_1Im^+$ cations as compared to the $C_2C_1Im^+$ counterpart. It is also interesting to note that the protonation of the imidazolium cation reduces the ionicity of the system, as reflected by lower $\Lambda_{imp}/\Lambda_{NMR}$ values. This may be a result of a stronger ion–ion interaction in protic ionic liquids, as also discussed by Miran *et al.*[36] Upon addition of water, the ionicity of the protic ILs increases suggesting that water is capable of interfering with the native cation–anion coulombic forces, consistently with the observed

cation–water interactions discussed above. By contrast, the ionicity of C_2C_1ImTFSI and C_2C_1ImTfO is much less affected by added water.

4 Conclusions

In this work we have investigated the transport properties of water–ionic liquid binary systems by performing PFG-STE NMR and conductivity measurements. To better understand how the molecular structure influences the local dynamics, we have investigated different ionic liquids with a systematic variation of aprotic/protic cations ($C_2C_1Im^+$ and C_2HIm^+) and more or less hydrophilic anions (TfO^- and $TFSI^-$). Overall, the addition of water enhances the mobility of all ionic species, which results in higher self-diffusion coefficients and ionic conductivities. However, the degree to which cation and anions are individually affected strongly depends on their molecular structure.

In C_2C_1ImTFSI, which is representative of hydrophobic and water immiscible ionic liquids, the dynamical effects are limited to a narrow concentration range, beyond which phase separation occurs. In this system, cations and anions are equally affected and no specific water–ion interaction is suspected. For its protonated counterpart, C_2HImTFSI, an associative diffusional behavior is detected for water and the cation at very low water concentrations, whereas at high water contents the imidazolium cation is speeded up more than the anion. By contrast, in C_2C_1ImTfO the anion is the species most affected at high water contents, while in C_2HImTfO both ions are affected in a similar way. These findings suggest preferential interaction sites for water that are the –NH group in protic ionic liquids and the $-SO_3$ group in the TfO anion, a scheme of interaction that can explain the selective self-diffusion enhancements that we observe. In protic ionic liquids the interaction between water and the –NH group on the imidazolium is manifested by proton exchange, which is much faster in C_2HImTfO as compared to C_2HImTFSI. Moreover, the analysis of the molar conductivity obtained by impedance measurements and from diffusion NMR reveals that the ionicity ($\Lambda_{imp}/\Lambda_{NMR}$) is lower in the protic ionic liquids than in the aprotic, in longer chain cations than in shorter, and for cations in association with TfO than with TFSI. This trend further proves the tendency for complexation once sites of interaction are provided.

Altogether these results represent a considerable step forward with respect to a better understanding of the structure–property relationship in water added ionic liquids. In addition, our results provide new and important indications for the design of ionic liquid based electrolytes in which the addition of water can selectively enhance the mobility of specific ionic species.

Acknowledgements

The financial support from the Chalmers' *Energy* and *Materials Science* Areas of Advance is kindly acknowledged. The Swedish NMR Centre is also acknowledged for providing the infrastructure for diffusion NMR experiments. The authors also thank Dr Romain Bordes for fruitful discussions and assistance in setting up the equipment for conductivity measurements. We also thank Dr Moheb Nayeri for rewarding discussions throughout the work.

References

1 M. Armand, F. Endres, D. R. MacFarlane, H. Ohno and B. Scrosati, *Nat. Mater.*, 2009, **8**, 621–629.
2 P. Lozano, *ChemSusChem*, 2010, **3**, 1359–1363.
3 J. R. O'Dea, N. J. Economou and S. K. Buratto, *Macromolecules*, 2013, **46**, 2267–2274.
4 B. Wang, *J. Power Sources*, 2005, **152**, 1–15.
5 L. Zhang, J. Zhang, D. P. Wilkinson and H. Wang, *J. Power Sources*, 2006, **156**, 171–182.
6 Y. Shao, G. Yin, Z. Wang and Y. Gao, *J. Power Sources*, 2007, **167**, 235–242.
7 Y. Kohno and H. Ohno, *Chem. Commun.*, 2012, **48**, 7119–7130.
8 M. Anouti, J. Jacquemin and P. Porion, *J. Phys. Chem. B*, 2012, **116**, 4228–4238.
9 K. Mori, T. Kobayashi, K. Sakakibara and K. Ueda, *Chem. Phys. Lett.*, 2012, **552**, 58–63.
10 T. Takamuku, Y. Kyoshoin, T. Shimomura and S. Kittaka, *J. Phys. Chem. B*, 2009, **113**, 10817–10824.
11 W. Li, Z. Zhang, B. Han and S. Hu, *J. Phys. Chem. B*, 2007, **111**, 6452–6456.
12 L. Cammarata, S. G. Kazarian, P. A. Salter and T. Welton, *Phys. Chem. Chem. Phys.*, 2001, **3**, 5192–5200.
13 J. P. Hallett and T. Welton, *Chem. Rev.*, 2011, **111**, 3508–3576.
14 P. Bonhôte, A.-P. Dias, M. Armand, N. Papageorgiou, K. Kalyanasundaram and M. Grätzel, *Inorg. Chem.*, 1998, **37**, 166.
15 Y. Kohno and H. Ohno, *Phys. Chem. Chem. Phys.*, 2012, **14**, 5063–5070.
16 M. Klähn, C. Stuber, A. Seduraman and P. Wu, *J. Phys. Chem. B*, 2010, **114**, 2856–2868.
17 P. Stange, K. Fumino and R. Ludwig, *Angew. Chem., Int. Ed.*, 2013, **52**, 2990–2994.
18 A. A. Niazi, B. D. Rabideau and A. E. Ismail, *J. Phys. Chem. B*, 2013, **117**, 1378–1388.
19 A. Menjoge, J. Dixon, J. F. Brennecke, E. J. Maginn and S. Vasenkov, *J. Phys. Chem. B*, 2009, **113**, 6353–6359.
20 A. L. Rollet, P. Porion, M. Vaultier, I. Billard, M. Deschamps, C. Bessada and L. Jouvensal, *J. Phys. Chem. B*, 2007, **111**, 11888–11891.
21 A. Stark, A. W. Zidell and M. M. Hoffmann, *J. Mol. Liq.*, 2011, **160**, 166–179.
22 J. E. Tanner, *J. Chem. Phys.*, 1970, **52**, 2523.
23 R. Mills, *J. Phys. Chem.*, 1973, **77**, 685.
24 M. S. Kelkar, W. Shi and E. J. Maginn, *Ind. Eng. Chem. Res.*, 2008, **47**, 9115–9126.

25 A. Martinelli, M. Maréchal, A. Ostlund and J. Cambedouzou, *Phys. Chem. Chem. Phys.*, 2013, **15**, 5510–5517.
26 H. Tokuda, K. Hayamizu, K. Ishii, M. A. B. H. Susan and M. Watanabe, *J. Phys. Chem. B*, 2004, **108**, 16593–16600.
27 S. M. Urahata and M. C. C. Ribeiro, *J. Chem. Phys.*, 2005, **122**, 024511.
28 M. Ue, A. Murakami and S. Nakamura, *J. Electrochem. Soc.*, 2002, **149**, A1385.
29 A. Noda, M. A. B. H. Susan, K. Kudo, S. Mitsushima, K. Hayamizu and M. Watanabe, *J. Phys. Chem. B*, 2003, **107**, 4024–4033.
30 J. W. Blanchard, J.-p. Beli, T. M. Alam, J. L. Yarger and G. P. Holland, *J. Phys. Chem. Lett.*, 2011, **2**, 1077–1081.
31 T. Singh and A. Kumar, *Vib. Spectrosc.*, 2011, **55**, 119–125.
32 A. Noda, K. Hayamizu and M. Watanabe, *J. Phys. Chem. B*, 2001, **105**, 4603–4610.
33 K. R. Harris, *J. Phys. Chem. B*, 2010, **114**, 9572–9577.
34 K. Hayamizu, S. Tsuzuki, S. Seki and Y. Umebayashi, *J. Chem. Phys.*, 2011, **135**, 084505.
35 H. Tokuda, S. Tsuzuki, M. A. B. H. Susan, K. Hayamizu and M. Watanabe, *J. Phys. Chem. B*, 2006, **110**, 19593–19600.
36 M. S. Miran, H. Kinoshita, T. Yasuda, M. A. B. H. Susan and M. Watanabe, *Phys. Chem. Chem. Phys.*, 2012, **14**, 5178–5186.
37 K. Ueno, H. Tokuda and M. Watanabe, *Phys. Chem. Chem. Phys.*, 2010, **12**, 1648.